

**IGF12 -XII Convegno Nazionale
Gruppo Italiano Frattura
Parma, 12-13 giugno 1996**

**FATIGUE CRACK GROWTH PREDICTION IN SPECIMENS SIMILAR TO
SPUR GEAR TEETH**

Adriano Blarasin¹, Mario Guagliano², Laura Vergani²

¹ Centro Ricerche FIAT, Strada Torino, 50 - Orbassano (TO)

² Dipartimento di Meccanica, Politecnico di Milano,
Piazza Leonardo da Vinci, 32 - Milano

ABSTRACT

The problem of the fatigue crack propagation in surface treated specimens similar to the gear teeth is dealt with. Experimental fatigue tests were carried out by means of carburized and carburized and shot peened specimens. In order to predict the crack propagation and to consider the effect of the treatments different models of the cracked specimens were realized. Two approaches were followed: the finite element and the weight function method. Three and two dimensional finite element models were constructed and the stress intensity factors were evaluated by considering the effect of the load and of the residual stresses, due to the treatments. These results were compared with the ones obtained by the weight function technique and the agreement found was good. The weight function was directly used in a software which allows crack propagation predictions, by considering the effect of the hardness and of the residual stresses. The comparison between these theoretical predictions and the experimental results validated the approach followed.

1. INTRODUCTION

Power transmissions using gear pairs result for each tooth in a cyclic loading, which may lead to the initiation of a fatigue crack in the fillet radius both in the pinion and in the driven gear. Once the crack is initiated the fatigue crack propagation phase may take a considerable part of the service life of gears till the 30%-40%, if the gears are carburized [1], [2], [3]. The crack propagation prediction is then important to accurately evaluate the total life of gears. This implies that some factors, difficult to be evaluated, were known.

The first one is the stress intensity factor of the cracked gear teeth. In fact, due to the shape and the loading modes, it is not possible use theoretical solutions and numerical

analyses are necessary to obtain reliable values of the stress intensity factor. The most widely used method is the finite element one: many procedures were developed to accurately reproduce the stress singularity at the crack tip and to have precise results in many different crack geometries and load application modes, even if they require extensive meshing work and considerable calculation time [4].

Other techniques allow easier calculations, for example the weight function technique leads to very fine results of the stress intensity factor both under mode I and under mode II loading [5].

Once the stress intensity factor has been determined it is also necessary to know the mechanical characteristics of the surface layer of the material. In fact, gears are subjected to surface treatment to improve their resistance both in terms of contact fatigue and of bending fatigue. It is note that these treatments cause hardening of the surface layers of the material and induce residual stress fields, compressive in the hardened layer. Both these two factors strongly affect the crack growth behaviour [6], [7], [8], [9]. Some authors [10], [11] proposed a modified expression of the Paris law in which the coefficient and the exponent are given as a function of the hardness of the material. They evaluated the residual stresses, difficult to be experimentally measured, by means of the hardness profiles and the crack growth rate by means of an effective stress intensity factor, ΔK_{eff} , determined taking into account both the applied stresses and the residual ones. In correspondence of a depth there is a hardness value and then a curve $\frac{da}{dN}$ versus

ΔK_{eff} . Once the hardness is known the actual crack growth rates may be obtained by considering the different stress intensity values at the different crack depths.

This approach was followed also in this study, but it was applied to a particular specimen (Brugger specimen) [12] which allows to reproduce the stress state of gears and it is usually utilized to quality control of gears under impact loading. In fact the experimental tests capable to verify the proposed propagation law are difficult to be performed on gears, requiring apposite facilities; furthermore they are generally expensive in terms of costs and time. For this reason it is interesting to look for simplified test procedures.

The stress intensity factors were numerically calculated by means of finite element models and of the weight function technique and the results were compared.

Theoretical predictions were verified by the experimental results from Brugger specimens and good agreement was obtained.

Besides these results were compared with data available in literature [13], [14], [15] in order to verify if the crack propagation test on Brugger specimens can substitute those on gears, with considerable saving of time and costs.

2. SPECIMENS AND MATERIAL

Experimental fatigue tests were conducted by using special specimens (shown in figure 1), which reproduce the stress and strain field of the gear teeth, but allow easier experimental tests. Brugger [12] drew the specimen in order to have the most stressed section as in a tooth; in figure 1 the most stressed section is found by considering the 30° inclined straight lines. The nominal stress is calculated:

$$S = \frac{P \cdot h \cdot 6}{b \cdot s^2} \quad (1)$$

where h , s are shown in figure and b is the thickness.

By entering the specimen dimensions [mm]

$$S = 0.049 \cdot P$$

The theoretical stress concentration factor, K_t , is equal to 1,57.

During the fatigue tests the central zone of the specimen is fixed and pulsating forces are applied on the specimen wings. The tests are interrupted when a wing is completely broken.

The specimen material is 18CrMo4 carburized; in table 1 the mechanical characteristics (experimentally determined) and the cyclic ones (from literature [16]) are shown.

All the specimens are carburized, some specimens were sanded and some specimens were shot peened after the carburizing treatment. Three groups of specimens were therefore considered: a) carburized, b) carburized and sanded, c) carburized and shot peened. The fatigue tests were conducted by means of all the specimen groups.

In table 2 the chemical composition of the 18CrMo4 is shown.

Table 1 Mechanical and cyclic characteristics of 18CrMo4

R_m [MPa]	R_{sn} [MPa]	A_5 [%]	E [GPa]	σ'_f [MPa]	ϵ'_f [m/m]	b	c	K' [MPa]	n'
1300	900	9	1.95	2344	0.27	-0.097	-0.398	2875	0.244

Table 2 Chemical composition of the 18CrMo4

C[%]	Si[%]	Mn[%]	P[%]	S[%]	Cr[%]	Ni[%]	Mo[%]
0.203	0.27	0.84	0.022	0.042	1.02	0.02	0.20

The characteristics of the carburizing treatment are similar to that ones utilized for the gears and are reported in table 3. The total time of the treatment is 340 minutes.

Table 3 Carburizing treatment characteristics

PHASE	TEMPERATURE [°C]
Heating	860
Carburizing and diffusing (methane +5%ammonium)	885
Soaking	840
Quenching in oil	100
Tempering	180

In figure 2 the hardness profiles, which were found by means of microhardness measurements, are shown. It is evident that the hardnesses are similar even if there is a different mechanical treatment after the carburizing. The surface hardness is about equal to 770HV and for all the specimens this is the maximum value too, in fact the hardness is always decreasing from the external until the core of the material. The external carburized layer dimension is equal about to 0.9mm.

The residual stresses were measured by means of a X-ray diffractometer and are shown in figure 3. Due to the specimen shape it was possible to release only the residual stresses perpendicular to the axis of the specimen; but it is possible to suppose the axial residual stresses equal to the measured ones [14]. The residual stresses are strongly influenced by the mechanical treatment, in fact the residual stress values, when there is the shot peening, are much larger than in the other cases.

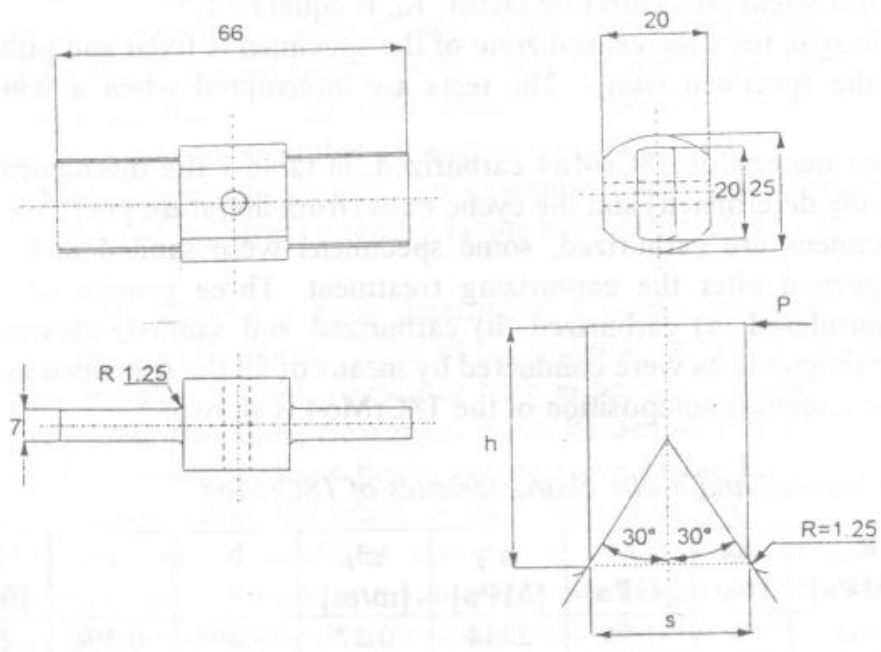


Fig. 1 Brugger specimen used for the fatigue tests and determination of the most stressed section.

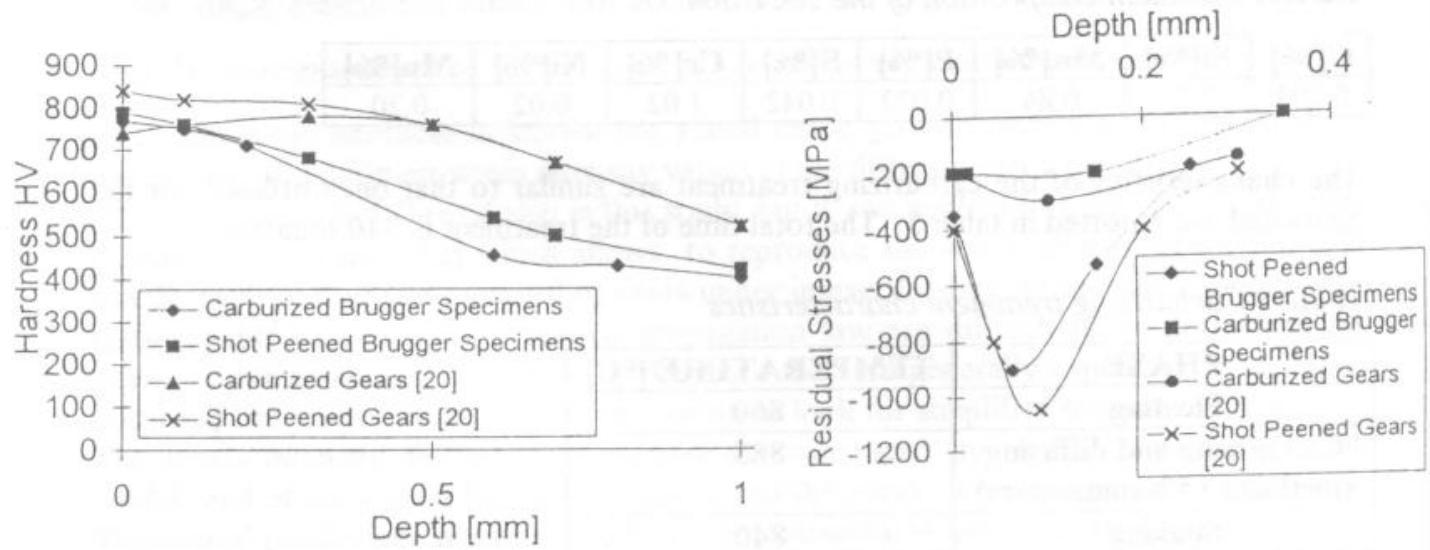


Fig. 2 Hardness profiles of the Brugger specimens and comparison with the reference [20] data from gears. Fig. 3 Longitudinal residual stresses of the Brugger specimens and comparison with the reference data [20] from gears.

3. NUMERICAL ANALYSES

Finite Element analyses

The problem of the stable crack propagation in a gear is not always a two dimensional problem: in fact, bearing in mind what it is possible to read in literature [2], only if the load is uniformly distributed on the tooth flank the crack development is well described by two-dimensional schematizations, while, if the load is concentrated only on one side of the tooth flank, the crack will have approximatively a quarter circle shape and will initiate at the corner of the specimen.

The simulation of this type of crack requires the development of three dimensional models and besides great care must be taken in modelling the crack front.

In fact the presence of the stress/strain singularity in the close neighbourhood of the crack tip requires the use of particular techniques to be correctly simulated. The most commonly used is the so called “quarter point technique”, which is applied to standard quadratic isoparametric elements and was object of many researches. However, the most recent studies in this field show that the presence of so distorted elements is not necessary if the mesh is sufficiently fine or if the Virtual Crack Extension method is used for the calculation of the J-Integral.

Two different finite element models were developed representing the most common type of fatigue cracks in gears. In figure 4a the model with a straight crack with a depth equal to 0.1mm, while in figure 4b the model with the quarter circle corner crack with a radius equal to 0.1 mm are shown. According to the experimental observations, for the first model the load was assumed uniform along the specimen width while in the second model the load was assumed to be concentrated at one end of the specimen in correspondence of the crack, which begins always from the most stressed point, as determined in figure 1.

Linear elastic analyses were executed and the trends of the shape factors β , defined as

$$\beta = \frac{K_I}{S\sqrt{\pi a}}$$

along the two crack fronts are shown in figure 5.

However, these finite element models are very expensive in terms of modelling and calculation time and the results can be mesh dependent, then it seems opportune to look for simplified two dimensional models. An approach of this type was successfully utilized by the authors for crankshafts [17] and now it is proposed for calculating the fracture mechanic parameters in the Brugger specimens.

Two dimensional models were carried out, see figure 6.

The two different crack geometries considered before were simulated with a plane strain model (straight crack $a=0.1\text{mm}$) and a plane stress model (corner crack $a=0.1\text{mm}$).

If the three-dimensional results are compared with the two-dimensional ones it can be noted that the plane strain β is very near to the value of the straight crack in its middle point, while the plane stress one is close to the surface corner crack results. So it can be affirmed that, as first approximation results, the β values obtained by the 2D analyses can be used to characterize two common types of cracks in Brugger specimens and gears.

It is possible to consider different crack depths by means of these 2D models, in fact they are substantially less exacting than the three-dimensional ones.

In figure 7 it is possible to observe the trend of the shape factors β till a crack depth equal to 1mm for the two-dimensional models.

To be sure of the reliability of the results the same models, but using focussed elements around the tip of a crack 0.1 mm deep were constructed and the results in terms of J-Integral compared; the differences were found to be negligible. In this way it is possible to validate the two dimensional schematization adopted, that makes use of no distorted elements, and to simulate the crack propagation by simply releasing the nodes lying on the opposite crack faces, without re-meshing the model every time.

The stress intensity factor was also calculated by extrapolating the values determined by using the nodal displacement on the open face of the crack: the differences are less than 2%. In this way it is also possible to separate the contribute of the I and the II mode of fracture: the results show that for small crack length the contribute of the II mode of fracture is negligible.

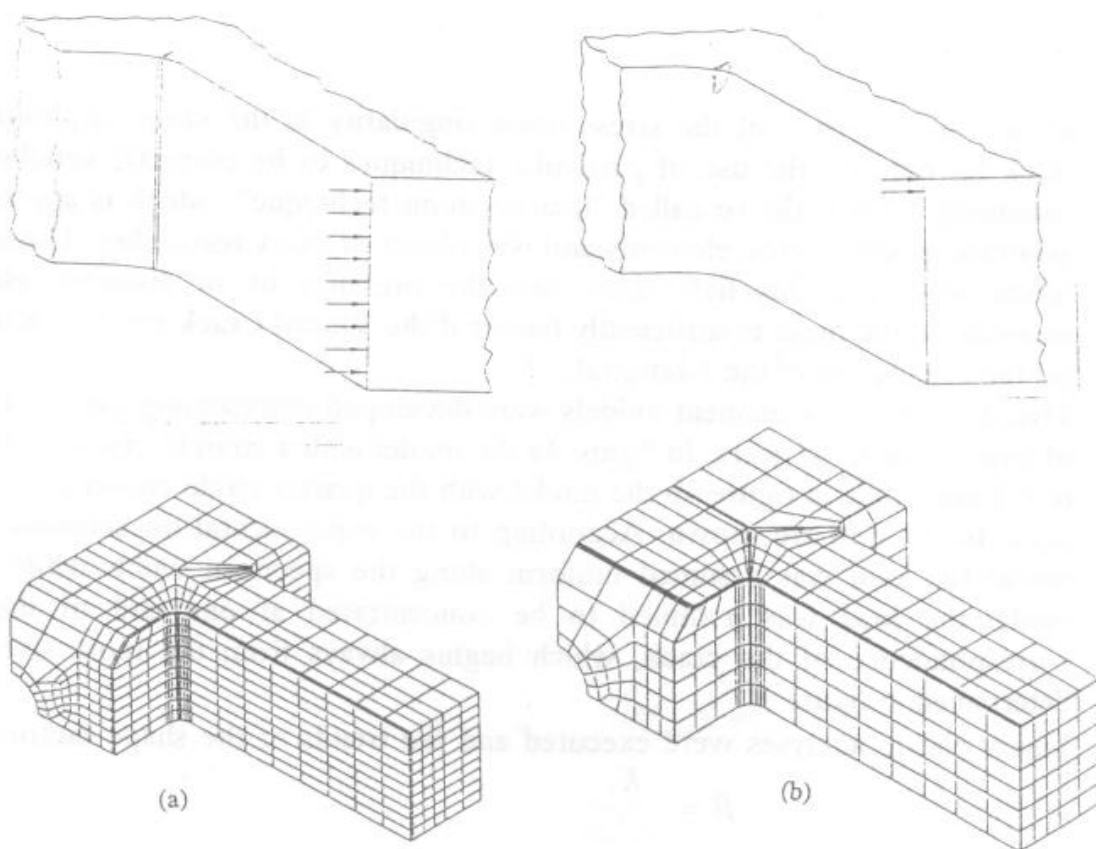


Fig.4 Three-dimensional finite element models: a) straight front crack ($a=0.1\text{mm}$); b) quarter circle corner crack ($a=0.1\text{mm}$).

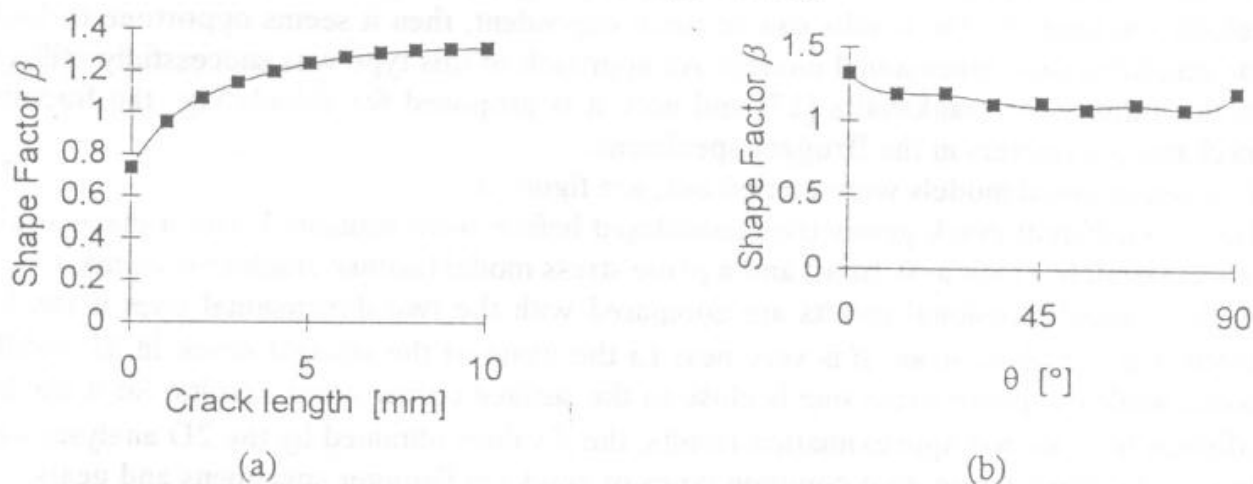


Fig.5 Shape factor β along the crack front for the three-dimensional finite element models: a) straight front crack ($a=0.1\text{mm}$); b) quarter circle corner crack ($a=0.1\text{mm}$).

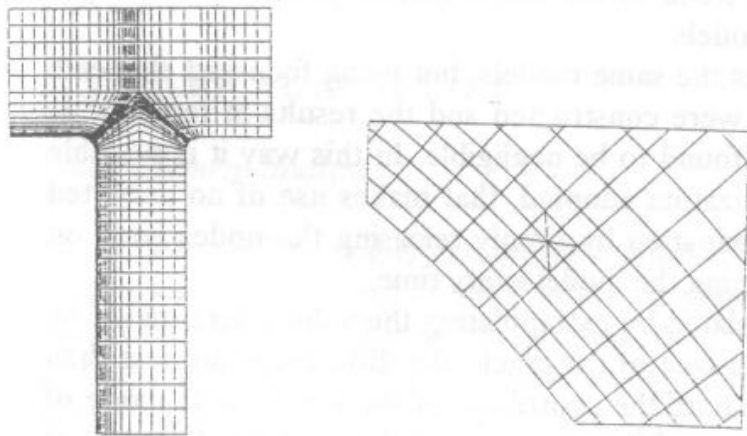


Fig.6 Two-dimensional finite element model

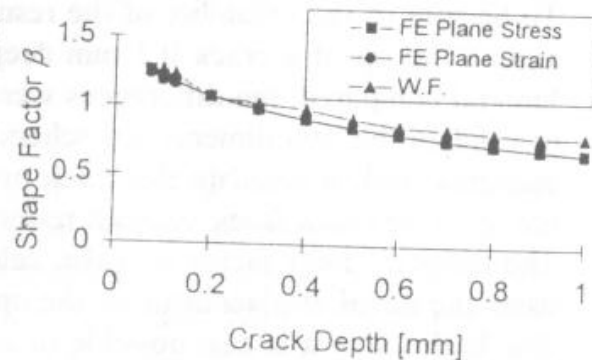


Fig.7 Shape factor β for the two-dimensional finite element models and weight function.

It is possible to consider the presence of a residual stress field and its evolution during the crack propagation. In this way it is possible to calculate the effective values of the stress intensity factor, which takes into account the effective stress state in the cracked specimen.

The residual stresses experimentally determined were introduced in the models, by using a numerical procedure based on thermal analysis [18].

In table 4 the values of the effective stress intensity factors, calculated for the carburized and carburized and shot peened specimens and for three different crack depths and with a $S=420$ MPa, which allows to evidence the different effect of the two treatments considered, are shown. It is clear the effect of the shot peening treatment in fact the resulting stress intensity factors are less than zero (with a nominal stress $S=420$ MPa). On the contrary the differences between the two types of cracks are not significant, as it was already seen by the β value trends. For this reason only the results referred to the plane strain condition are shown.

Table 4 Stress intensity factors by the finite element models ($S=420$ MPa)

Depth [μm]	Carburizing [MPa $\sqrt{\text{mm}}$]			Carburizing and shot peening [MPa $\sqrt{\text{mm}}$]		
	K_I load	K_r residual	K_{eff} effective	K_I load	K_r residual	K_{eff} effective
75	253	-97	156	253	-369	-116
100	283	-111	173	283	-422	-139
125	307	-135	172	307	-452	-145

Weight Functions analyses

The method used for calculating the stress intensity factor in cracked gear teeth is the weight function technique [3], [4], which is ever more used for its computational efficiency and engineering accuracy.

The mode I stress intensity factor is given for an edge crack by:

$$K_I = \int_0^a \sigma(x)m(x, a)dx$$

where $m(x, a)$ is an appropriate weight function of the cracked tooth and a unique property of the specimen geometry and $\sigma(x)$ is the stress distribution acting on the perpendicular to the crack plane and including both the stresses due to the applied load and the residual ones.

A similar formulation can be found for the II mode of fracture.

The advantage of this type of approach is that once the weight function is known it is not necessary further work of numerical modelling for analysing different crack depths. The main approximation is that there is not analytical weight function for the gear tooth and it must be numerically calculated. Alternatively, a known weight function of a specimen with a geometry similar to that of the gear tooth can be used.

In this study, the weight function of a prismatic notched bar [19] of finite width W is used:

$$m((x, a) = \frac{2}{\sqrt{2\pi a(1-\rho)}} [1 + M_1(1-\rho) + M_2(1-\rho^2)]$$

where a is the crack depth, x is the coordinate with the origin at the edge of the bar, $\rho=x/a$ and

$$M_1=0.6147+17.1944\alpha^2+8.7822\alpha^4$$

$$M_2=0.2502+3.2899\alpha^2+70.0444\alpha^4$$

with $\alpha=a/W$.

This geometry has yet been used for the analysis of cracked gears, giving reliable results: being the geometry of the Bruggen specimen even more similar to that of a prismatic bar, the results will be closer to the actual values. A similar weight function can be used for the II mode of fracture but it has been not considered because of its negligible influence on fatigue crack propagation in its early stage

A software based on the weight function technique was developed and the values of β calculated: in figure 7 the values of the shape factor β (in absence of residual stresses) are shown and compared with those obtained with the finite element models.

In table 5 the effective stress intensity factors evaluated by the weight function method and a nominal stress $S=420$ MPa are shown. If we compare these results with those of table 4 the agreement is good with a maximum difference of 6%, except the case of the shortest crack.

Table 5 Stress intensity factors by weight function ($S=420$ MPa)

	Carburizing [MPa√mm]	Carburizing and shot peening [MPa√mm]
Crack depth[μm]	K_{eff} effective	K_{eff} effective
75	147	-74
100	165	-131
125	179	-145

In figure 8 the effective stress intensity factor trends with respect to the crack depth and the maximum stress ($\sigma_{max}=K_t \cdot S$) are shown. It is evident the influence of the shot peening in particular in the hardened layer, till a crack depth of about 0.2mm.

4. LIFE PREDICTIONS AND EXPERIMENTAL RESULTS

In order to predict the life of the Bruggen specimens the following equations proposed by Kato and Deng [10], [11] were utilized:

$$\frac{da}{dN} = \frac{C}{(1-a^n)} (\Delta K_{eff}^n - \Delta K_{th}^n) \quad \Delta K_{th} \leq \Delta K_{eff} \leq \Delta K_c$$

$$\frac{da}{dN} = \frac{C}{(1-a^n)} \left(\frac{\Delta K_{eff}^n K_{fc}^n}{\Delta K_{fc}^n - \Delta K_{eff}^n} \right) \quad \Delta K_c \leq \Delta K_{eff} \leq K_{fc} \quad (2)$$

$$a = \frac{\Delta K_{th}}{K_{fc}} \quad K_c = (\Delta K_{th} K_{fc})^{1/2} \quad \frac{da}{dN} = \left[\frac{mm}{cycle} \right] \quad \Delta K = [MPa\sqrt{m}]$$

The unknown parameters were evaluated by the hardness values:

$$\begin{aligned} \Delta K_{th} &= 2.45 + 3.41 \cdot 10^{-3} H \\ K_{fc} &= 141 - 1.64 \cdot 10^{-1} H \\ n &= 4.31 - 8.66 \cdot 10^{-3} H + 1.17 \cdot 10^{-5} H^2 \\ \log C &= -10.0 + 1.09 \cdot 10^{-2} H - 1.40 \cdot 10^{-5} H^2 \end{aligned} \quad (3)$$

The software based on the weight function technique was used in order to have directly the prediction of the specimen life, by means of the equations (2).

In this software the nucleation crack phase is considered too. Due to the lack of experimental data relating to the nucleation of cracks in carburized materials the data available in literature were considered (see table 2). These data were determined from a material similar to that one used and the Coffin-Manson parameters were found by considering cracks of 0.05 mm depth. For this reason, in the software, until a depth of 0.05 mm the nucleation law is used, and after this value the propagation law is considered.

The calculations are interrupted when the cracks are equal to 1 mm, in fact the subsequent propagation rate is very high and the corresponding duration is not significant with respect to the total life of the specimens. Besides due to the presence of the II mode propagation, which increases by increasing the crack depth [6], the propagation direction changes and it would be necessary consider this mode too.

In figure 9 the crack growth rates obtained by means of the software are shown. It can be noted the influence of the treatments: a) is referred to the core material without residual stresses; b) is referred to the carburized material with its corresponding hardness and residual stresses; c) is referred to the carburized and shot peened material. (In this phase the sanded specimens were not considered because their results were between the other ones.)

It is possible to find the influence of the shot peening treatment on the threshold value of the stress intensity factors, in fact for the carburized specimens the value $\Delta K_{th} = 4.6$

MPa \sqrt{m} is found, on the contrary for the carburized and shot peened specimens $\Delta K_{th} = 5.2$ MPa \sqrt{m} .

In figure 10 the different trends (a-N) are shown. In the case of shot peened specimens the residual stresses cause retard in the crack propagation in the hardened and compressed layer, on the contrary out of this region the rate rapidly increases. In the case of carburized specimens this retard is not evident.

In figure 11 the predicted lifes were shown and compared with the experimental results, carried out by applying forces pulsating from 0 to a maximum value (R=0) on all the Brugger specimen types.

The experimental results show the treatment influences, in fact the fatigue strength (nominal stress) increases from S=550 MPa (carburized specimens) to S=730 MPa (carburized and sanded specimens) and to S=870 (carburized and shot peened specimens).

The agreement between the experimental and the prediction data is good. In particular the predictions are finer when the crack propagation takes a long part of the total life, on the contrary if the nucleation phase is more important the error is larger, due to the uncertainty of the nucleation data. The shot peened specimen predictions are close to the experimental data because the limit of 0.05 mm between the nucleation and the propagation is probably actual, due to the large compressive residual stresses. In fact the ΔK_{eff} is close to the ΔK_{th} value, when a=0.05mm.

On the contrary in the other cases, with the same a , ΔK_{eff} is larger than ΔK_{th} and a large part of propagation is spent before the limit considered of 0.05mm. In order to have more precise predictions it would be to have experimental data about the nucleation of this material.

In figure 12 the fractography of a fracture section of a carburized specimen is shown: a) is the hardened layer zone and it is evident a brittle, intergranular fracture, on the contrary b) is the core zone and the high strained grains are evident.

5. COMPARISON WITH GEAR FATIGUE TESTS

The experimental tests were conducted by means of Brugger specimens, which reproduce the stress field of a tooth. Besides it is possible to find that the hardness profiles and the residual stress distributions in the Brugger specimens are similar to that ones revealed in the teeth, realized by the same material and subjected to the same treatments; see figures 2, 3, where the differences between the curves are within the typical 10% error of the HV measurements.

Kato and alter [10] determined the stress intensity factor trend from a gear of the same fillet radius as the Brugger specimens and of a similar carburized material. In figure 8 this trend is compared with those obtained by Brugger specimens, the agreement is good.

6. CONCLUSIONS

Specimens similar to gear teeth were realized in order to conduct simpler and less expensive experimental tests. These specimens, which reproduce the stress and strain field of the gears, were constructed by 18CrMo4 carburized and the hardness profiles and the residual stress trends are similar to that ones measured in the gears.

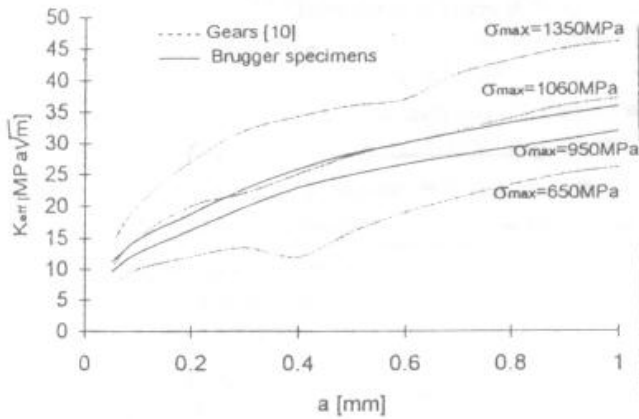
By means of these specimens it was possible to conduct a great number of fatigue experimental tests and to study the crack propagation in carburized materials.

The following conclusions can be drawn:

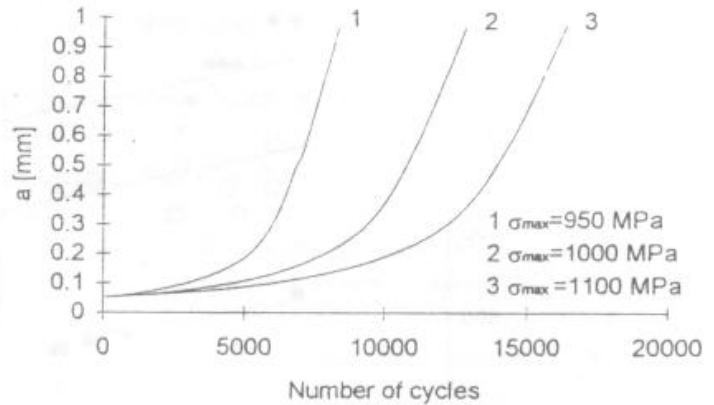
- 1) three groups of specimens (carburized, carburized and sanded, carburized and shot peened) were experimentally tested and the influence of the different treatments were evidenced;
- 2) three-dimensional finite element models of the cracked specimens were realized; the stress intensity factors were evaluated for two different cracks, one with a constant depth along the thickness and one circular on one side of the specimen. To simplify the analysis two-dimensional models were constructed. Due to the good agreement between the results of the different models, the two-dimensional ones were utilized to evaluate the trend of the stress intensity factor with respect to the crack depth. The influence of each treatment was evaluated by introducing the corresponding residual stresses in the numerical models. The effective stress intensity factors were calculated. The differences between the two different cracks are not evident. All the following calculations are therefore conducted considering a straight front crack;
- 3) weight function method was utilized to determine in a simpler way the stress intensity factors of the cracked specimens. These results are in good agreement with the finite element ones;
- 4) a software, based on the weight functions, was realized. By means of the equations proposed by Kato and alter it was possible to predict the specimen crack propagation. The obtained propagation laws show the great influence of the hardened layer on the

crack growth rate. The predicted lives are close to the experimental ones and the deviation found may be attributed to the nucleation data.

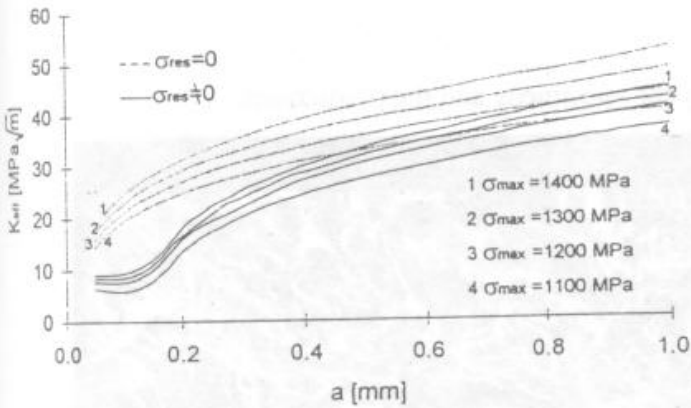
5) all the results obtained by these specimens were compared with corresponding data available in literature and obtained by gears. The good agreement found shows that these specimens simulate in an accurate way the gear behaviour.



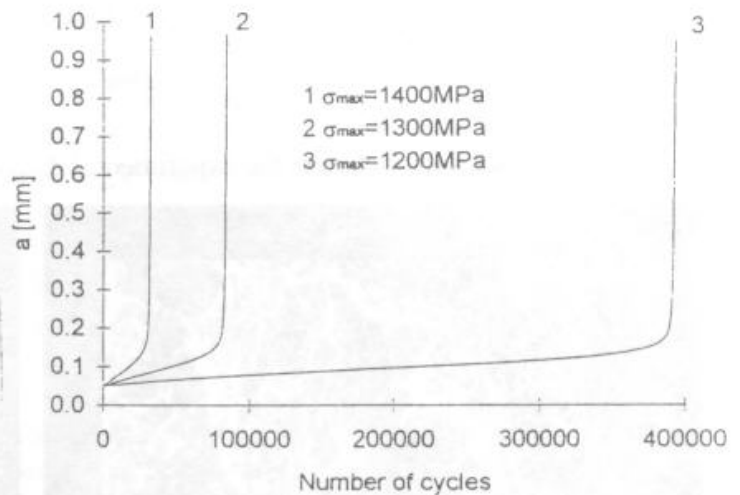
(a)



(a)



(b)



(b)

Fig.8 Effective stress intensity factor (weight function method :a)carburized specimens; b)shot peened specimens ($\sigma_{res} \neq 0$) and not treated specimens ($\sigma_{res} = 0$).

Fig.10 Crack propagation prediction: a) carburized specimens; b) carburized and shot peened specimens.

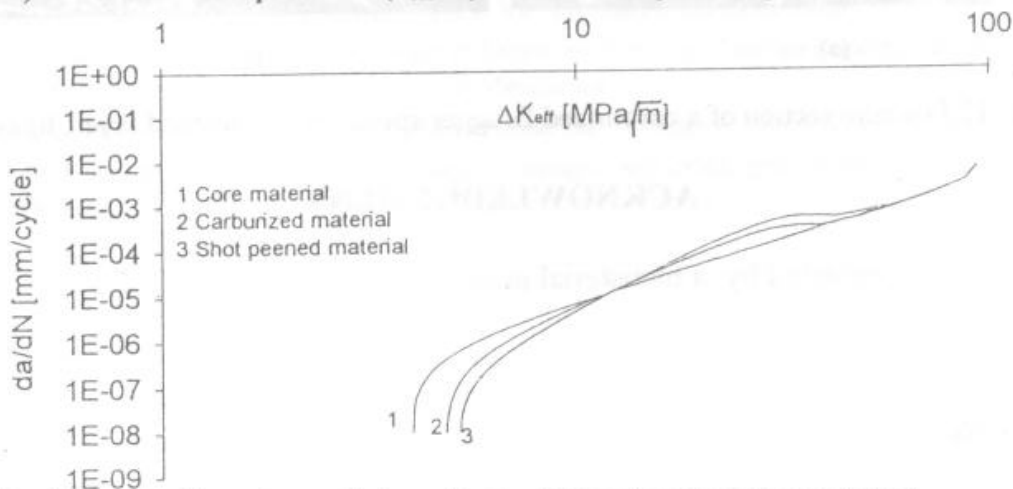


Fig.9 Crack propagation rate predictions for the different materials considered.

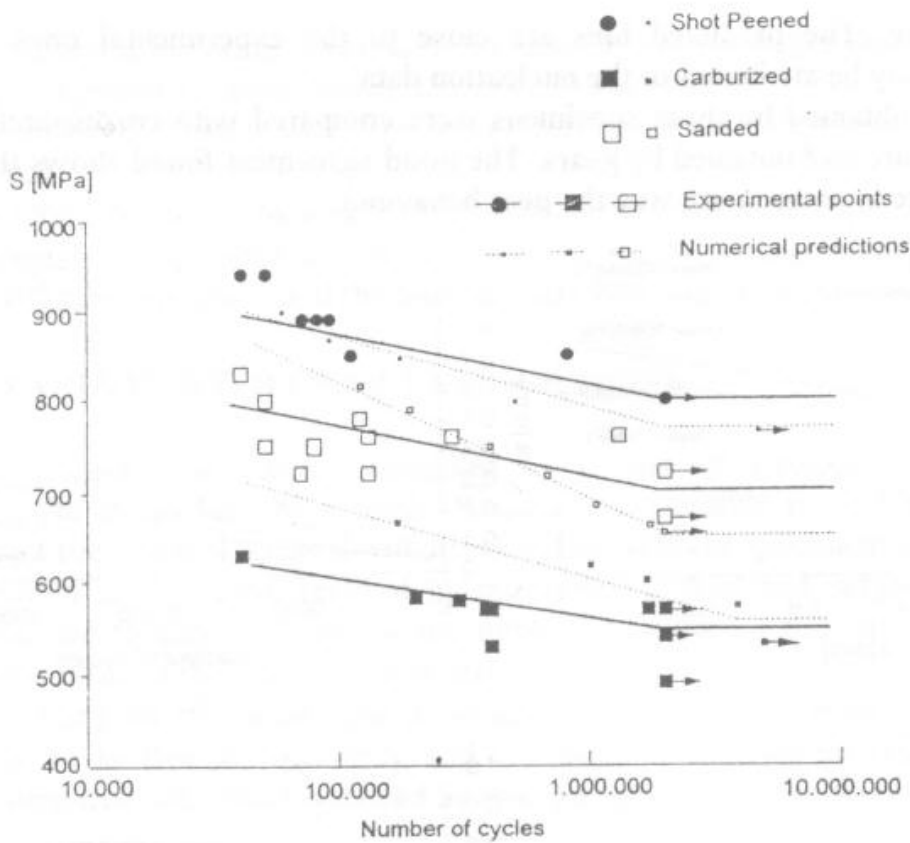


Fig.11 Comparison between the experimental data by the specimens and the predictions.

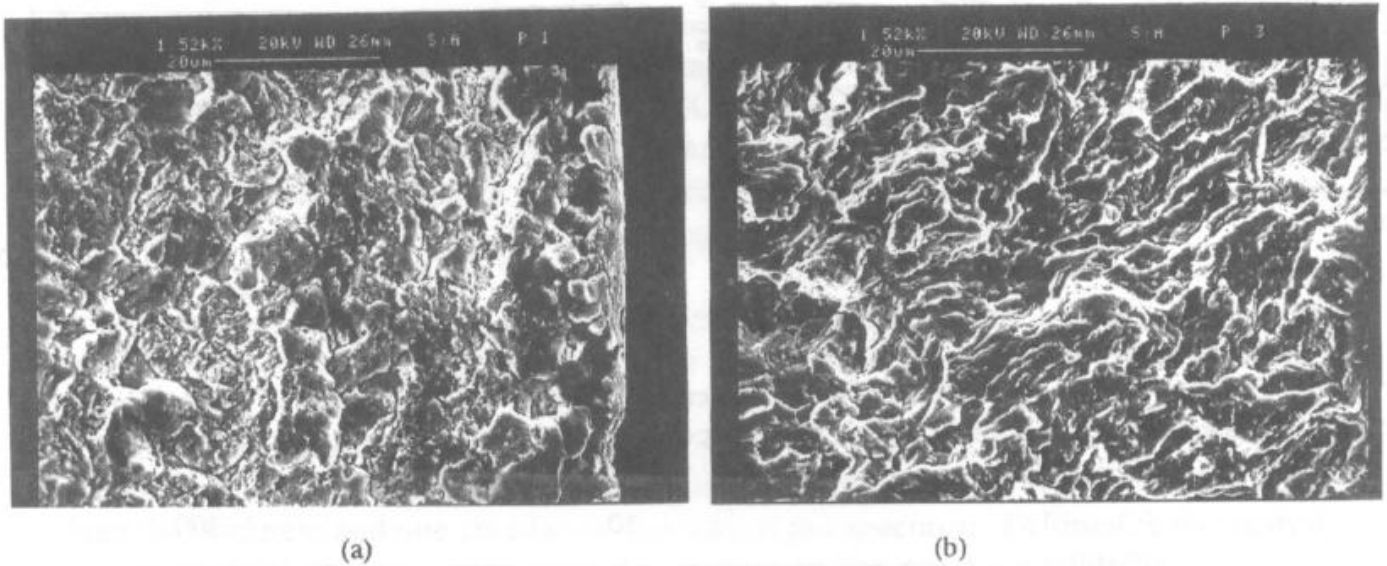


Fig.12 Fracture section of a carburized Bruggen specimen: a)hardened layer; b) core.

ACKNOWLEDGEMENT

This study was supported by a ministerial grant.

REFERENCES

1. R.W. Landgraf, R.H. Richman (1975) Fatigue Behavior of Carburized Steel. *Fatigue of Composite Materials, ASTM STP 569*, pp.130-144.

2. S.Pehan, T.K. Hellen, J.Flašker (1995) Applying Numerical Method for Determining the Service Life of Gears. *Fatigue Fract. Engng Mater. Struct.* Vol.18, No.9, pp.971-979.
3. G.Nicoletto (1993) Approximate Stress Intensity Factors for Cracked Gear Teeth. *Engineering Fracture Mechanics.* Vol.44, No.2, pp.231-242.
4. B.Aberšek, J.Flašker (1995) Numerical Method for Evaluation of Service Life of Gears. *International Journal for Numerical Methods in Engineering.* Vol.38, pp.2531-2545.
5. B.Aberšek, J.Flašker (1994) Stress Intensity Factor for Cracked Gear Tooth. *Theoretical and Applied Fracture Mechanics* 20, pp.99-104.
6. A.Yoshida, K.Fujita, T.Kanehara, K.Ota (1986) Effect of case Depth on Fatigue Strength of Case-hardened Gear. *Bulletin of JSME.* Vol.29, No.247, pp.228-234.
7. B.Jeong, M.Kato, K.Inoue, N.Takatsu (1992) The bending Strength of Carburized Fine Module Gear Teeth. *JSME International Journal. Series III,* Vol.35, No.1, pp.136-141.
8. K.Nagamura, Y.Terauchi, S.Y.Martowibowo, K.Terayama (1992) Study on Gear Bending Fatigue Strength Design Based on Reliability Engineering. *JSME International Journal. Series III,* Vol.35, No.1, pp.142-151.
9. K.Nagamura, Y.Terauchi, S.Y.Martowibowo (1994) Study on Gear Bending Fatigue Strength Design Based on Reliability Engineering. *JSME International Journal. Series C,* Vol.37, No.4, pp.795-803.
10. M.Kato, G.Deng, K.Inoue, N.Takatsu (1993) Evaluation of the Strength of Carburized Spur Gear Teeth Based on Fracture Mechanics. *JSME International Journal. Series C,* Vol.36, No.2, pp.233-240.
11. K.Inoue, S.Lyu, G.Deng, M.Kato (1996) Fracture Mechanics Based Evaluation of the Effect of the Surface Treatments on the Strength of Carburized Gears. *Proc. VDI Berichte.* NR.1320, pp.357-369.
12. H.Brugger (1970) Schlagbiegeversuche zur beurteilung einsatzgehaeterer stahle. *Schweizer Archiv.* Vol.36, pp.219-226.
13. T.Tobe, M.Kato, K.Inoue, N.Takatsu, I.Morita (1986) Bending Strength of Carburized SCM420H Spur Gear Teeth. *Bulletin of JSME.* Vol.29, No.247, pp.273-286.
14. K.Inoue, T.Maehara, M.Yamanaka, M.Kato (1989) The Effect of Shot Peening on the Bending Strength of Carburized Gear Teeth. *JSME International Journal. Series III,* Vol.32, No.3, pp.448-454.
15. S.R.Daniewicz (1991) Conception and Development of Improved Analytical Prediction Models for Fatigue Induced Tooth Breakage Due to Cyclic bending in Spur Gear Teeth. Ph. D. Dissertation, The Ohio State University.
16. G.M.Newaz (1981) Axial Cyclic Response of Unnotched and Notched Carburized Cylindrical Members under Constant Amplitude Completely Reversed Loading. *FCP Report No.41,* College of Engineering University of Illinois at Urbana-Champaign.
17. M.Guagliano, L.Vergani (1994) A Simplified Approach to Crack Growth Prediction in a Crankshaft. *Fatigue Fract. Engng Mater. Struct.* Vol.17, No.11, pp.1295-1306.
18. A.Barberini, G.Iussich (1996) Propagazione di Difetti in Elementi Trattati Superficialmente. Tesi di Laurea, Politecnico di Milano, Dipartimento di Meccanica.
19. H.F.Bückner (1971) Weight Function for the Notched Bar. *Z. Angew. Math. Mech.* 51, pp. 97-109.
20. K.Inoue, M.Kato, M.Yamanaka (1989) Fatigue Strength and crack growth of carburized and shot peened spur gears. *Proc Power Transmission Engineering Conference (ASME),* pp. 663-668.